Blue-Green Systems

Blue-Green Systems Vol 3 No 1, 201 doi: 10.2166/bgs.2021.120

Coupled nitrogen transformation and carbon sink in the karst aquatic system: a review

Wenwen Chen[a], Huanfang Huang[b], Haixiang Li[a], Jianhua Cao[c], Qiang Li[c], Yingjie Chen[d], Bing Bai[c] and Honghu Zeng[a,*]

[a] Collaborative Innovation Center for Water Pollution Control and Water Safety in Karst Area, Guilin University of Technology, Guilin 541004, China
[b] South China Institute of Environmental Sciences, Ministry of Ecology and Environment, Guangzhou 510535, China
[c] Key Laboratory of Karst Dynamics of Ministry of Land and Resources, Institute of Karst Geology, Chinese Academy of Geological Sciences, Guilin 541004, China
[d] State Key Laboratory of Biogeology and Environmental Geology, China University of Geosciences, Wuhan 430074, China
*Corresponding author. E-mail: zenghonghu@glut.edu.cn

ABSTRACT

Carbonate bedrock regions represent that 14% of Earth's continental surface and carbon (C) sink in karst water plays an important role in the global C cycle due to the CO_2 consumption during carbonate mineral weathering. Intensive agriculture and urbanization have led to the excessive input of nitrogen (N) into aquatic systems, while the high concentrations of inorganic C in the karst water might affect the N cycle. This paper summarized the characteristics of water in karst regions and discussed the N transformation coupled with the C cycle in the condition of high Ca^{2+} content, high pH, and high C/N ratios. Carbonates can consume more atmospheric and pedologic CO_2 than non-carbonates because of their high solubility and high rate of dissolution, resulting in the higher average CO_2 sink in karst basins worldwide than that in non-karst basins. Therefore, carbonate mineral weathering and aquatic photosynthesis are the two dominant ways of CO_2 absorption, which are termed as coupled carbonate weathering. As the alkalinity and high C/N content of karst water inhibit the denitrification and mineralization processes, the karst aquatic environment is also served as the N sink.

Key words: atmospheric CO_2 sink, bicarbonate, carbonate weathering, karst water, nitrogen cycle

HIGHLIGHTS

- Karst aquatic systems contain high contents of DIC, Ca^{2+}, Mg^{2+}, and high pH.
- C–N cycles in the karst aquatic systems are mainly related with DIC and NO_3^-.
- Enhanced nitrification and DIC can promote aquatic communities growth.
- Atmospheric CO_2 sink in carbonate area is high.

1. INTRODUCTION

1.1. Karst evolution and the urgency of carbon balance

The term 'karst' refers to regions that typically developed from carbonate rocks. These rocks mainly include mineral calcite ($CaCO_3$) and mineral dolomite ($CaMg(CO_3)_2$), containing limestone and dolomite rock or dolostone, respectively (Hartmann 2015). Carbonate bedrock regions represent 14% of Earth's continental surface, including broad swaths of southwestern China. The southwestern China karst region is one of the largest globally continuous karst areas, covering $\sim 540 \times 10^3$ km^2 over eight provinces (Zhang *et al.* 2020). Carbonate karst aquifers serve as the drinking water source for about one-quarter of the global population (Ford & Williams 1989).

Stress on climate change due to carbon dioxide (CO_2) emissions has increased significantly in recent decades, which is attributed to deforestation, the change of land-use type, and the use of fossil fuels (Melnikov & O'Neill 2006). Liu *et al.* (2015) estimated that China's cumulative carbon (C) emission during 2000–2013 was nearly 2.9 gigatons, which was larger than China's estimated total forest sink during 1990–2007 (2.66 gigatons of C). Moreover, this estimated C sink was still undervalued in terms of deserts and karst formations. In China, two considerable challenges for estimating C sink are the amount of CO_2 emitted and absorbed by the landscape.

As limestone degradation could be a substantial inorganic C sink, the C sink in the karst area might play an important role in the global C cycle and the balance of China's C emission.

1.2. The important role of carbon sink in karst water

Water plays a critical role in the C cycle in the karst area, as it is a basic medium to transform derived organic and inorganic carbon, and C can also be exchanged with the atmosphere in the form of CO_2 across the water–air interface. Previous studies have shown that many non-karst (mainly silicate area) rivers are usually supersaturated with CO_2, then leading to the emissions of CO_2 (Butman & Raymond 2011; Wang *et al.* 2011; Rasilo *et al.* 2017). However, in karst water, such as rivers, lakes, and reservoirs, carbonate mineral weathering consumes CO_2 with a more rapid ratio and, therefore, increases the concentrations of dissolved inorganic carbon (DIC) (mainly HCO_3^-) (Berner 2003; Liu *et al.* 2011). As DIC can be consumed by aquatic phototrophs by photosynthesis and transformed to organic C in inland water, the absorption of CO_2 continues and forms karst C sink rapidly (Liu *et al.* 2011). Therefore, it is of great importance to understand the role of karst processes as a global C sink and the quantification of C fluxes.

1.3. Excessive input of nitrogen (N) in karst water

Intensive agriculture and urbanization have led to the excessive input of N into the soil and further increased the amount of nitrate (NO_3^-) in water (Xin *et al.* 2019), as well as changed the N cycle process in the aquatic ecosystem. Human activities have delivered 64 Tg N/yr to rivers and streams in the 20th century, which doubled that in the 19th century (34 Tg N/yr) (Beusen *et al.* 2016). It has been shown that the cycling of C and N in karst aquatic systems is closely related to each other, as coupled C–N cycling is involved in the transformation of DIC into dissolved organic carbon (DOC) (Zhao *et al.* 2021). The increasing anthropogenic atmospheric CO_2 emissions result in a progressive increase in N limitation in plants. C sequestration and increased atmospheric CO_2 concentrations would lower terrestrial N availability and lead to decreases in N flux to the atmosphere and N deposition to aquatic ecosystems. As industrial and agricultural discharge drives a sharp increase in anthropogenic N emissions, the magnitude of N from this anthropogenic input will likely become large enough to sustain similar conditions of ecosystem N availability (McLauchlan *et al.* 2013). The elevated DIC concentrations in karst water may also enhance the aquatic photosynthetic uptake of DIC (Liu *et al.* 2010b, 2011) and then may promote N translation. However, the interactions between N translation and CO_2 absorption in karst aquatic ecosystems have not been well depicted.

1.4. Objectives

In this review, we provide an overview of the relevance of karst regions to the special water characteristics and discuss the impact on the N transformation due to these specific water characteristics. We (1) start with an introduction to the characteristics of karst water, (2) present an overview of N transformation in karst water systems, (3) discuss the processes related to carbon sink, and (4) show the challenges and new directions in karst water C/N balances.

2. CHARACTERISTICS OF KARST WATER

2.1. The characteristic of carbonate weathering

The carbonate weathering is formulated as $CaCO_3 + CO_2 + H_2O \leftrightarrow HCO_3^- + Ca^{2+}$ and $CaMg(CO_3)_2 + 2CO_2 + 2H_2O \leftrightarrow 4HCO_3^- + Ca^{2+} + Mg^{2+}$. CO_2 consumed during carbonates dissolution would finally be released to the atmosphere by the precipitation of carbonates in the oceans (Berner *et al.* 1983), and the kinetics of dissolution is much faster as compared to precipitation considering the ocean turnover time (timescales of <3 ka). Therefore, carbonate weathering is critical in global CO_2 balances (Van Cappellen & Qiu 1997; Kump *et al.* 2000).

CO_2 was absorbed by raindrops formed in the atmosphere, and of which the concentration would further increase after precipitation and infiltration in the soil due to vegetation and microbial processes. Furthermore, the CO_2 in soil water could dissolve the bedrock underlying soil, composed of carbonate rock, during percolation of soil moisture in the karst area. Previous research found that the contribution of carbonates, e.g. HCO_3^-, to the total dissolved load in the lakes and rivers worldwide was up to 38% (Ferris *et al.* 1994).

2.2. High contents of HCO_3^-, Ca^{2+}, and Mg^{2+} in alkaline karst water

The rapid process of carbonate weathering resulted in remarkably higher concentration of bicarbonate and calcium in water in carbonate terrains as compared to silicate terrains (Liu & Dreybrod 1997; Liu *et al.* 2007; Raymond *et al.* 2008). Therefore, the reaction between carbonate minerals and CO_2, which increases DIC ($DIC = CO_2(aq) + HCO_3^- + CO_3^{2}-$) concentrations, may impact the C cycle and represent a net sink of atmospheric CO_2 in a short time scale (Martin 2017).

Previous studies in Table 1 showed that the karst water pH values ranged from 6.45 to 9.7, with pH in most of the water samples higher than 7. Considering dissolved CO_2 is mainly present as HCO_3^- (Liu *et al.* 2018) when the water pH varies from 6.5 to 10, the main form of DIC in karst water is HCO_3^- and the conversion of HCO_3^- to CO_2 is slow. While the HCO_3^- concentration varies in different karst water samples, with the values ranging from 12.2 to 2,633 mg/L, the HCO_3^- concentration in karst water is much higher than that in non-karst water of similar environmental parameters (e.g. temperature and precipitation). In addition, great variations of Ca^{2+} and Mg^{2+} concentrations were also observed. In terms of geographic locations, the concentrations of HCO_3^-, Ca^{2+}, and Mg^{2+} in South China were higher than those in North China, which could be attributed to the differences in environmental parameters, such as temperature, lithology, and climate. As can be seen in Table 1, the concentrations of HCO_3^-, Ca^{2+}, and Mg^{2+} in a typical karst catchment in Guangxi, China were about 10 times higher than that in the Yellow River. Therefore, it is summarized that karst water is typically with high contents of HCO_3^-, Ca^{2+} and Mg^{2+}, and high pH.

2.3. C/N ratio in karst river and non-karst water

As shown in Table 2, the organic carbon (OC)/N ratio in karst water in the upstream of the Pearl River (11.8:1) is about twice compared to that in the Pearl River estuary (5.0:1) (Liu *et al.* 2020). While the organic carbon can be

Table 1 | The concentrations (in mg/L) of HCO_3^-, Ca^{2+}, and Mg^{2+} in karst water and other water types

Locations	pH	HCO_3^-	Ca^{2+}	Mg^{2+}	References
Karst water					
Groundwater, southwest China	7.33–7.36	190.22–335.92	45.60–71.46	12.60–35.14	Liu *et al.* (2007)
Reservoir water, Guizhou, China	7.88	166.53	68.90	–	Liu *et al.* (2021)
Spring water, southwest China	7.08–7.52	184.04–273.84	62.72–93.87	0.27–2.34	Liu *et al.* (2004)
Reservoir water, Guizhou, China	7.25–9.18	–	24.74–74.09	5.54–19.01	Ma *et al.* (2021)
Karst catchment, Guangxi, China	–	270.00–2,633.00	122.00–1,382.00	20.00–176.00	Sun *et al.* (2021)
Spring water, Guizhou, China	7.50–9.7	90.1–255.30	24.30–61.00	9.10–21.60	Chen *et al.* (2017)
Lijiang River Basin	6.45–8.52	21.96–201.00	5.80–53.36	0.98–8.73	Sun *et al.* (2019)
Guancun River, Guangxi, China	–	173.90–289.04	71.14–86.04	4.81–14.37	Cheng *et al.* (2012)
Karst spring-fed pool, Chongqing, China	–	–	52.50–56.00	1.80–2.10	Jiang *et al.* (2013)
Groundwater, Shandong, China	7.57	263.78	158.59	26.06	Wu *et al.* (2021)
Groundwater, Jianghan Plain, China	6.60–7.50	439.00–748.00	85.00–140.00	20.00–43.00	Zhou *et al.* (2013)
Groundwater, North China Plain	–	12.20–1,879.50	2.40–1,622.20	–	Zhang *et al.* (2013a)
Non-karst water					
River water, Guangdong, China	7.73–7.95	–	37.67–131.36	6.57–276.97	Chen *et al.* (2019)
Yellow River, China	8.11–8.21	186.66–208.01	86–94	29.76–46.80	Zhang *et al.* (1995)
Hanfeng Lake, Chongqing, China	8.05–8.12	65.453–67.466	–	–	Zhao *et al.* (2021)
Mixed water					
Tibetan lakes, China	7.80–10.40	ND–9,613.00	4.33–1,140.00	1.80–9,089.00	Li *et al.* (2016)
Ichetucknee River water, USA	7.48–8.06	2.86–2.93	1.34–1.40	0.29–0.30	Montety *et al.* (2011)

ND, not detected.

Table 2 | Organic C/N ratios reported in some world large rivers, modified based on Liu *et al.* (2020)

Rivers/ reservoirs	DOC/N	References
Karst water		
Pearl River (pristine upstream)	11.8:1	Liu *et al.* (2020)
Longtan Reservoir, Tian'e, China	7.13:1[a]	Cao *et al.* (2019)
Wulixia Reservoir, Guilin, China	1.11:1[b]	Song *et al.* (2017)
Runoff in the Puding Country, China	6–9:1[c]	Song *et al.* (2019)
Non-karst water		
Superior Lake (Canada, Ontario)	8.13:1	Zigah *et al.* (2012)
Amazon River	29.1:1	Meybeck (1982)
Pearl River estuary	5:1	Liu *et al.* (2020)
Yangtze River	6.2:1	Wu *et al.* (2007)
Yellow River estuary	6.0:1	Liu *et al.* (2012), Zhang *et al.* (2013b)
Mississippi River estuary	20.4:1	Dagg *et al.* (2005)
Yenisei River	43.1–52.4:1	Holmes *et al.* (2012)

[a]Dissolved inorganic carbon was used.
[b]TOC was used here.
[c]Dissolved carbon was used.

categorized into DOC and particulate organic carbon based on a size threshold of 0.2 μm. A previous study showed that the DOC/N ratio in a karst reservoir in Guilin, China was 1.11:1 (Song *et al.* 2017), which is not consistent with aforementioned Liu *et al.*'s work. Moreover, the OC/N ratio values in karst soil were slightly lower than those in non-karst soil (Gu *et al.* 2018). In addition, Table 2 also shows that the DOC/N ratios in rivers of China are much lower than those in the Mississippi River estuary and Yenisei River, probably due to high precipitation and high organic matter (OM) inputs, indicating that the OM might be the key factor influencing the DOC/N ratio in rivers as riverine OM is with high DOC/N ratio (about 30:1) (Bauer *et al.* 2013).

Neither the data of the DIC/N ratio in the karst or the non-karst aquatic systems are available. The DIC contents in karst water are relatively higher as discussed before; therefore, it can be deduced that the total concentrations of carbon including DIC and DOC in karst water are also higher than those in non-karst water. As organisms translate DIC into total organic carbon (TOC) by photosynthesis, theoretically the total carbon (TC)/N ratios in karst water should also be higher. Considering the limited number of researches available currently, more researches are still required to figure out the differences of TC/N ratios between karst and non-karst water.

3. TRANSFORMATION OF NITROGEN IN KARST WATER

3.1. Nitrogen emission in karst aquatic systems

As one of the most important cycles in water systems, the N cycle, including the conversion and flux of N, has received worldwide attention in recent years. Human activities, such as intensive agriculture and rapid urbanization, lead to excessive and repetitive N inputs, which significantly affect the natural cycle of N. In the 20th century alone, human activities have increased the amount of N delivering to rivers and streams from 34 to 64 Tg N/yr (Beusen *et al.* 2016). N pollution has become one of the most concerned and prevalent environmental problems, especially in karst areas. Karst areas are subjected to greater pressure of N pollution than other regions because karst aquifers are particularly sensitive and vulnerable to chemical pollution from human activities due to their developed networks of fractures, pipelines, and sinkholes (Jiang 2013).

In water systems, the two sources for N are natural and artificial activities. While biological N fixation was the only important process in Earth's ecosystems producing reactive N to support C fixation into energy-rich OM (primary production) before the agricultural and industrial revolutions, human activities have been introducing large amounts of N into the environment through municipal sewage, industrial effluent, and agriculture since the agricultural and industrial revolutions (Wakida & Lerner 2005), especially the N fertilizer used in agriculture to promote crop growth and increase crop yield (Wang *et al.* 2019a, 2019b).

3.2. N cycle processes

In aquatic environments, N was composed of organic and inorganic N (Nie *et al.* 2018). The organic nitrogen is divided into dissolved organic nitrogen (DON) and particulate organic nitrogen (PON), depending on whether it can pass through a 0.2-μm filter (Jørgensen 2009). DON includes a variety of organic molecules and compounds, ranging from small molecules like urea and amino acids, to peptides and proteins, while PON includes both dead OM and living organisms that are larger than 0.2 μm (Jørgensen 2009). The inorganic nitrogen in aquatic ecosystems includes dissolved N_2 gas, oxidized ions such as nitrate (NO_3^-), nitrite (NO_2^-), ammonium ion (NH_4^+), and ammonia gas (NH_3) (Howarth 2009). The most frequently detected mineral N fractions in water are NO_3^- and NH_4^+, which are also the dominant components of N produced by human activities (Beusen *et al.* 2016).

In water systems, N would go through a variety of bacteria-mediated processes, mainly including nitrogen fixation, mineralization, nitrification, denitrification, dissimilated nitric acid reduction to ammonium, and ammonia oxidation (Figure 1). Most N on Earth is in the form of N_2, which becomes biologically significant after being fixed by bacteria, lightning, volcanic activity, and human activity. In aquatic environments, N fixation is mostly carried out by heterotrophic or autotrophic bacteria and cyanobacteria. NO_3^-, NO_2^-, NH_4^+, and NH_3 are the active N in water. Algae, rooting plants, fungi, and bacteria absorb and reduce NO_3^- and NO_2^- to NH_4^+ in a process known as assimilative nitrate or nitrite reduction. NH_4^+ could be catalytic-oxidized by nitrifying bacteria to NO_3^- in a process called nitrification, from which the nitrifying bacteria gain energy to fix CO_2 into new bacterial biomass. Plants, algae, and microorganisms use nitrates and ammonium to produce organic nitrogen-containing compounds, which could be further taken up by animals through the food chain, through one of the following processes: direct absorption, assimilation, and reduction. The organic N eaten by animals or decomposed by microorganisms is excreted as ammonium or as urea which is further rapidly hydrolyzed to ammonium. In addition, NO_3^- is also reduced by heterotrophic or autotrophic bacteria to NO_2^-, which is further reduced to N_2 by a process known as traditional denitrification or dissimilated nitrate reduction. These processes that release N from organic N back to the environment are called nitrogen mineralization. The other N cycle processes include denitrification based on chemosynthetic oxidation of sulfides or reduced iron (Howarth 2009), anaerobic oxidation of ammonia to N_2 (Anammox), dissimilatory reduction of NO_3^- to NH_4^+ via NO_2^- (DNRA) (Medinets *et al.* 2015), and autohydrogenotrophic denitrification of NO_3^-/NO_2^- to N_2. However, the relative importance of these newly discovered processes in water systems remains quite uncertain (Howarth 2009).

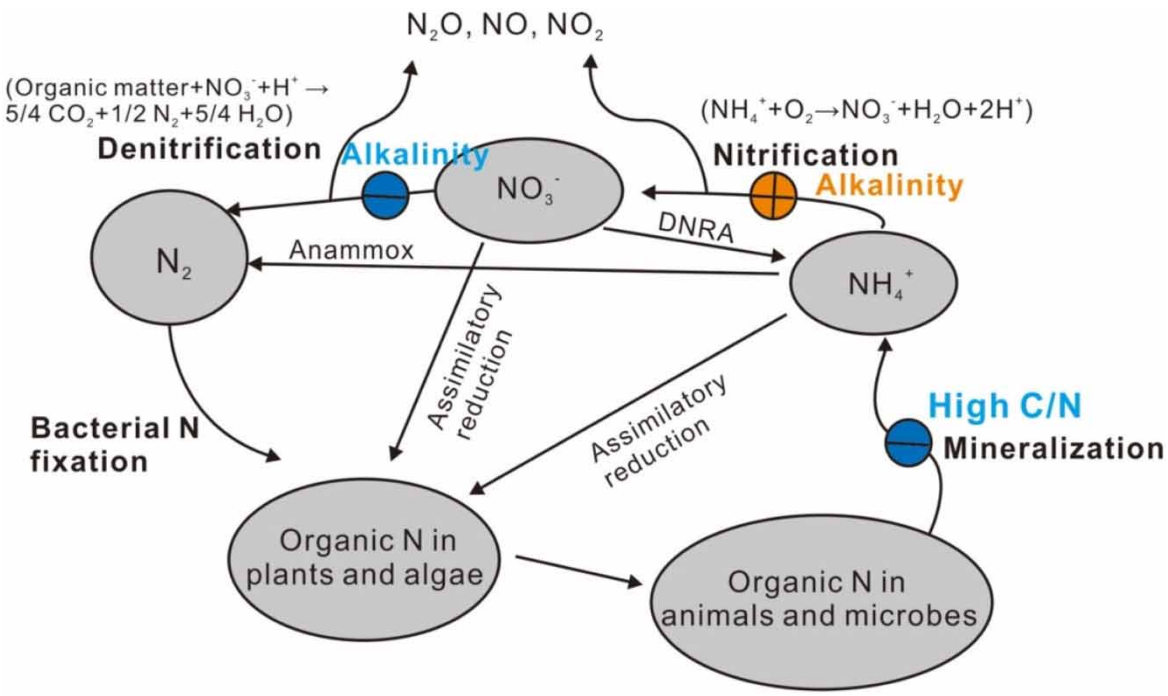

Figure 1 | The simplified N cycle in the karst water system (based on Howarth 2009). The plus sign suggests that alkaline karst water promotes the nitrification process. Minus signs indicate that the high C/N content and alkalinity in karst water inhibit the mineralization and denitrification processes.

3.3. N cycle characteristics in karst area

Due to the unique hydrochemistry of karst water (such as high Ca^{2+} content, high pH, and high DIC concentrations), the N cycle characteristics in karst areas are different from those in non-karst areas. In the perspective of the N cycle, the alkalinity and high DIC contents in karst areas can inhibit the heterotrophic denitrification and mineralization processes, which determine the karst aquatic environment as an N sink. During nitrification, the oxidation of every ammonium ion produces two protons worth of acidity and makes the environment more acidic (Howarth 2009). Therefore, the alkaline environment in karst water is beneficial to neutralizing the acid generated by nitrification and further promotes nitrification. However, the denitrification process is opposite to nitrification. Every nitrate ion consumed during denitrification consumes one proton of acidity, and thus, this process tends to raise the pH of the environment (Howarth 2009). Consequently, the inherent alkalinity of karst water will inhibit the denitrification reaction. Furthermore, the high DIC/N ratios in karst water can inhibit the gross mineralization because microbes immobilize rather than mineralize N to maintain the stoichiometric ratio of DIC/N in their biomass (Xin *et al.* 2019).

3.4. Cycling of C and N in karst area

The cycling of C and N in aquatic environments is closely related, with coupled control of organic carbon concentrations through aquatic biological processes of assimilation or denitrification (Gruber & Galloway 2008; Zeng *et al.* 2019). Although there are few studies on the C–N coupling cycle in karst water systems, some studies have found that excessive nitrogen emissions from human activities lead to the C–N coupling cycle participating in the carbonate weathering process, resulting in the increase of DIC flux in karst water systems (Raymond *et al.* 2008; Jiang 2013; Zhao *et al.* 2020). Most biological processes in water systems are C-limited processes, but this is not the case in karst aquatic environments. As shown in Figure 2, in karst water systems, higher DIC and increased NO_3^- concentration due to the enhanced nitrification and human activities can promote the growth of aquatic communities (Liu *et al.* 2018; Zeng *et al.* 2019). The growing amount of algae and microorganisms in water increases the consumption of DIC and NO_3^- through photosynthesis, as the conversion of DIC to OC by photosynthesis induces the consumption of NO_3^-, and therefore, reduces the NO_3^- concentration (Pedersen *et al.* 2013; Nõges *et al.* 2016; Liu *et al.* 2018). In addition, during this process, DIC and NO_3^- are converted to OM and O_2 is released, which contrasts with the traditional knowledge that CO_2 is released during carbonate precipitation (Jiang 2013). It has been shown that in the Lijiang River water, the consumption of DIC and NO_3^- by aquatic photosynthesis was in a ratio of 9:1 (mol/mol) to produce autochthonous DOC (Zhao *et al.* 2021). To sum up, the C–N cycle coupled with DIC and NO_3^- promotes the generation of in-situ DOC in karst aquatic environments, which constitutes the relatively long-term natural C and N sinks in karst water systems, as shown in Figure 2.

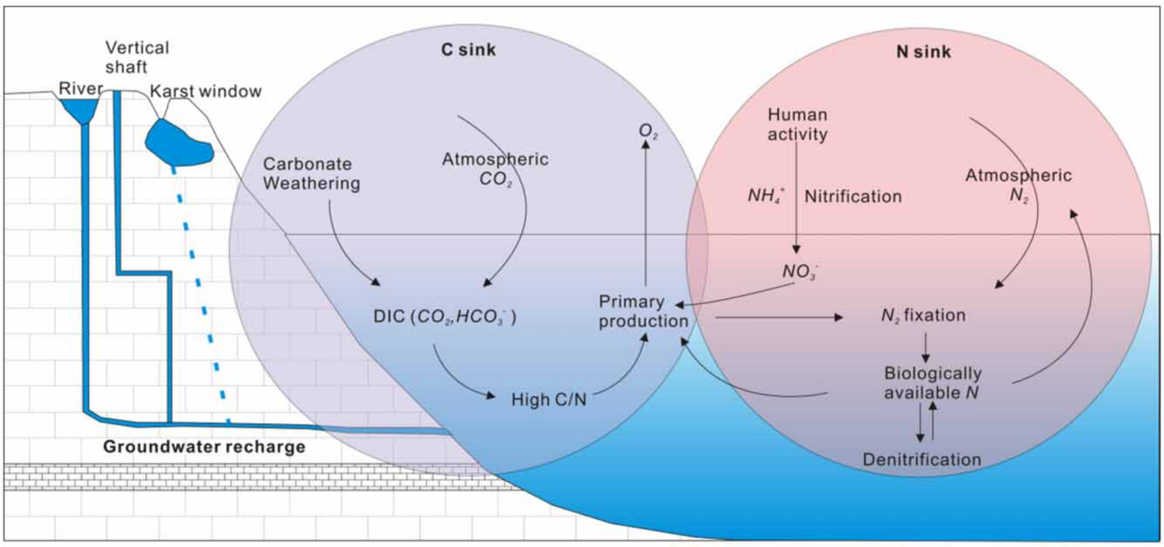

Figure 2 | The characterized C–N cycle in karst water systems. Plus signs indicate that those processes are promoted in the karst aquatic system and the minus sign implies the prohibited process.

4. THE PROCESSES RELATED TO CARBON SINK IN KARST WATER

4.1. The global carbon budget and carbonate CO_2 sink volume

Five major components in the global C budget are fossil CO_2 emissions (E_{FOS}), emissions from land-use change (E_{LUC}) (mainly deforestation), atmospheric CO_2 (G_{ATM}), ocean CO_2 sink (S_{OCEAN}), and terrestrial CO_2 sink (S_{LAND}). Over the last decade (2010–2019), E_{FOS} and E_{LUC} were 9.6 $\pm$ 0.5 and 1.6 $\pm$ 0.7 Pg·C/yr, respectively, G_{ATM} was 5.1 $\pm$ 0.02 Pg·C/yr, S_{OCEAN} and S_{LAND} were 2.5 $\pm$ 0.6 and 3.4 $\pm$ 0.9 Pg·C/yr, respectively, and the imbalance budget (B_{IM}) was -0.1 Pg·C/yr (Friedlingstein *et al.* 2020). The accepted values for S_{LAND} at present range from 1.8 to 3.4 Pg·C/yr in the global C budget (Melnikov & O'Neill 2006; Lal 2008; Friedlingstein *et al.* 2020). Similarly, another research indicated that S_{LAND} was calculated at 2.6 Pg·C/yr, while CO_2 sink due to photosynthesis and CO_2 emissions from plant respiration were 14.1 and 11.6 Pg·C/yr, respectively (Yuan & Liu 2003).

A large C sink is missing from the global carbon cycle with the value of 1.7–2.5 Pg·C/yr (Cao *et al.* 2011). CO_2 sink from carbonate might be an important component missed in previous studies; however, the volume of CO_2 sink by carbonate weathering on continents varied greatly in different researches, with its volume ranging from 0.018 to 0.6 Pg·C/yr worldwide, which is about 7–36% of the missing C sink (Yuan 1997; Gaillardet *et al.* 1999; Gombert 2002; Liu *et al.* 2010b). Liu *et al.* (2011) found that carbonate weathering contributed about 94% to the atmospheric CO_2 sink, while only 6% resulted from silicate weathering. More researches on CO_2 absorption experiments using more accurate calculation methods are still needed to estimate the atmospheric CO_2 sink by carbonate weathering.

4.2. Carbonate-related atmospheric CO_2 sinks

Two primary processes related to global sinks of atmospheric CO_2 are the transformation of CO_2 to HCO_3^- in water due to rock weathering (Li *et al.* 2011) and the assimilation of CO_2 by photosynthesis to organic C (Sabine *et al.* 2004; Zeebe & Caldeira 2008). There are three sources of HCO_3^-, including carbonate weathering by carbonic acid, carbonic weathering by sulfuric and/or nitric acids, and silicate weathering. Carbonates can consume more atmospheric and petrologic CO_2 because of their high solubility and high dissolution rate (Liu *et al.* 2010b), resulting in aquatic photosynthesis is the main process for CO_2 absorption in silicate terrains. The roles of both carbonate mineral weathering and aquatic photosynthesis, termed as coupled carbonate weathering, are significant in karst areas (Liu *et al.* 2018). In addition, Sun *et al.* (2021) also observed that the average contributions made by silicate weathering to the CO_2 sink in the Lijiang River basin ranged from only 2.3 to 14.8%, which indicated that carbonate weathering was the main source of HCO_3^- in this basin although carbonate rock area (3,832 km^2) is smaller than silicate rock area (5,482 km^2).

DIC is mainly consumed by phototrophs in aquatic ecosystems such as rivers, lakes, and the oceans (Dean & Gorham 1998; Cassar *et al.* 2004; Tortell *et al.* 2008). During this process, DIC is transformed in the water to OC and pCO_2 is reduced, which results in the continuous uptake of atmospheric CO_2 (Liu *et al.* 2010b). The biological productivity of aquatic phototrophs has been found to be associated with the supply of DIC from rock weathering. For instance, the utilization of HCO_3^- by *Oocystis solitaria Wittr* in karst water was 4.6-fold higher than that in non-karst water (Liu *et al.* 2010a).

Previous researches concluded that the atmospheric CO_2 consumed by carbonate weathering was compensated by a CO_2 released from marine carbonate precipitation over a relatively short time. However, this conclusion neglected the large amount of atmospheric CO_2 uptake during aquatic photosynthesis (Liu *et al.* 2010b). Moreover, Liu *et al.* (2018) also observed that the increased DIC concentration controlled by carbonate weathering in the karst area might enhance aquatic photosynthesis, promoting the consumption of atmospheric carbon. Therefore, the amount of CO_2 absorbed by the C sink in the karst area was larger as compared to other areas.

4.3. High carbon sink rate in carbonate area

As shown in Table 3, the range of carbon sink rate in carbonate area was 1.54–73 tC/km^2/yr, while in silicate area the range of this value was 0.02–8.0 tC/km^2/yr. The annual average C sequestration flux of limestone weathering in China was estimated to be 4.28–5.02 tC/km^2/yr (Li *et al.* 2019). The C sinks produced by carbonate weathering and the 'biological C pump' in the Li River basin were 12.17 and 2.24 tC/km^2/yr, respectively (Sun *et al.* 2021). The average amount of CO_2 consumed by C sinks in karst basins around the world (8.5 tC/km^2/yr) was about three times higher than that in non-karst basins (2.86 tC/km^2/yr). In karst water, the C sink is enhanced by N

Table 3 | The carbon sink rates (in $tC/km^2/yr$) in the different basins

	C sink rate	Silicate weathering	Carbonate weathering	References
Lijiang river, China	14.41		12.17	Sun *et al.* (2021)
Guancun Underground Stream, China	73.00			Pu *et al.* (2017)
Guancun Underground Stream, China	12.34			Guo *et al.* (2011)
Mumei Underground Stream, China	31.44			Guo *et al.* (2011)
Banzhai Underground Stream, China	11.80			Guo *et al.* (2011)
Pearl River basin, China			11.68	Cao *et al.* (2011)
China (2000–2014)			4.28	Li *et al.* (2019)
Taiwan, China	27.15			Li *et al.* (2019)
Karst zone, Southeastern China	8.56			Jiang *et al.* (2011)
Karst zone, North China	1.54			Jiang *et al.* (2011)
Karst zone, Qinghai-Tibetan plateau, China	2.20			Jiang *et al.* (2011)
Pearl River, China		7.40		Qin *et al.* (2015)
Pearl River basin, China	35.98			Wei (2003)
Yangtze River, China			11.27	Zhang *et al.* (2016)
Yangtze River, China			10.07	Li *et al.* (2019)
Yellow River, China			5.74	Li & Zhang (2003)
Yellow River, China			2.65	Li *et al.* (2019)
Xijiang River, China			11.06	Yang *et al.* (2020)
Russia		0.08		Zhang *et al.* (2021)
Canada		0.18		Zhang *et al.* (2021)
United States		0.49		Zhang *et al.* (2021)
Round the world		0.02–8.00		Gaillardet *et al.* (1999)

translation, as the concentration of dissolved CO_2 was decreased dramatically (about 75%) due to the increase of NO_3^- in the Yangtze River (Wang *et al.* 2007). Therefore, in the karst basin, the transformation of C and N by aquatic phototrophs was coupled.

5. CONCLUSIONS AND OUTLOOKS

Carbonate bedrock regions represent 14% of the continental surface of the Earth and provide drinking water resources for about 25% of the global population. C sink in karst water plays an important role in the global C cycle due to the CO_2 consumption during carbonate mineral weathering. This review highlights the consumption of CO_2 during carbonate weathering and the relevance of the N and C cycles in karst regions. Existing concentrations of HCO_3^-, Ca^{2+}, Mg^{2+}, and C/N ratios are presented, followed by a review of previous studies.

Here we show that,

1. Karst aquatic systems are characterized by high contents of HCO_3^-, Ca^{2+}, Mg^{2+}, high pH, and high C/N ratios.
2. The cycling of C and N in karst aquatic environments is closely related and the high content of DIC in karst systems will increase the nitrogen sink. Also, the growth of aquatic communities was promoted by higher concentration of DIC and the increase of NO_3^- due to the enhanced nitrification and human activities.
3. The budget of CO_2 sink from carbonate ranged from 0.018 to 0.6 Pg·C/yr (about 7–36% of the missing carbon sink), which indicated that carbonate weathering was an important component neglected in previous studies.
4. The range of C sink rates in carbonate area was 1.54–73.00 $tC/km^2/yr$, while in silicate area the range of this value was 0.02–8.00 $tC/km^2/yr$.

The N input in karst areas worldwide would increase due to continuous population growth, industrial activities expansion, and lifestyle improvement. This necessitates the collection of sufficient information about the C and N sinks in karst systems to provide reliable projections of C and N balances. As few studies are available specifically focusing on the impact of karst characteristics on the C sink as well as the N cycle, more field observations targeting the relationships between C and N cycles in karst aquatic systems are urgently needed to figure out the mechanism of N sink in karst water with high abundance of DIC.

ACKNOWLEDGEMENTS

This work was supported by the National Natural Science Foundation of China (No. 42067048, 41807387, and 42007310), Guangxi Foundation for Program of Science and Technology Research (No. 2020GXNSFAA159169), and Guangxi 'Bagui Scholar' Construction Project and Guangxi Science and Technology Planning Project (No. GuiKe-AD18126018).

DATA AVAILABILITY STATEMENT

All relevant data are included in the paper or its Supplementary Information.

REFERENCES

Bauer, J. E., Cai, W.-J., Raymond, P. A., Bianchi, T. S., Hopkinson, C. S. & Regnier, P. A. G. 2013 The changing carbon cycle of the coastal ocean. *Nature* **504**, 61–70. https://doi.org/10.1038/nature12857.

Berner, R. A., Kasaga, A. C. & Garrels, R. M. 1983 The carbonate-silicate geochemical cycle and its effect on atmospheric carbon dioxide over the past 100 million years. *American Journal of Science* **283**, 641–683.

Berner, R. A. 2003 The long-term carbon cycle, fossil fuels and atmospheric composition. *Nature* **426**, 323–326. https://doi.org/10.1038/nature02131.

Beusen, A. H., Bouwman, A. F., Van Beek, L. P., Mogollón, J. M. & Middelburg, J. J. 2016 Global riverine N and P transport to ocean increased during the 20th century despite increased retention along the aquatic continuum. *Biogeosciences* **13**, 2441–2451.

Butman, D. & Raymond, P. A. 2011 Significant efflux of carbon dioxide from streams and rivers in the United States. *Nature Geoscience* **4**, 839–842. https://doi.org/10.1038/ngeo1294.

Cao, J., Yang, H. & Kang, Z. 2011 Preliminary regional estimation of carbon sink flux by carbonate rock corrosion: a case study of the Pearl River Basin. *Chinese Science Bulletin* **56**, 3766–3773. https://doi.org/10.1007/s11434-011-4377-3.

Cao, Y., Yuan, R., Jiao, S., Zhang, Q. & Deng, F. 2019 Spatial distribution patterns of dissolved carbon and nitrogen based on semi-vatiration in Longtan Reservoir. *Yellow River* **41**, 94–99.

Cassar, N., Laws, E. A., Bidigare, R. R. & Popp, B. N. 2004 Bicarbonate uptake by Southern Ocean phytoplankton. *Global Biogeochemical Cycles* **18**. https://doi.org/10.1029/2003GB002116.

Chen, B., Yang, R., Liu, Z., Sun, H., Yan, H., Zeng, Q., Zeng, S., Zeng, C. & Zhao, M. 2017 Coupled control of land uses and aquatic biological processes on the diurnal hydrochemical variations in the five ponds at the Shawan Karst Test Site, China: implications for the carbonate weathering-related carbon sink. *Chemical Geology* **456**, 58–71. https://doi.org/10.1016/j.chemgeo.2017.03.006.

Chen, Y., Huang, H., Ding, Y., Chen, W., Luo, J., Li, H., Wu, J., Chen, W. & Qi, S. 2019 Trace metals in aquatic environments of a mangrove ecosystem in Nansha, Guangzhou, South China: pollution status, sources, and ecological risk assessment. *Environmental Monitoring and Assessment* **191**, 629. https://doi.org/10.1007/s10661-019-7732-5.

Cheng, Z., Jinliang, W., Junbing, P. & Jun, Y. 2012 Bicarbonate daily variations in a karst river: the carbon sink effect of subaquatic vegetation photosynthesis. *Acta Geologica Sinica – English Edition* **86**, 973–979. https://doi.org/10.1111/j.1755-6724.2012.00721.x.

Dagg, M. J., Bianchi, T. S., Breed, G. A., Cai, W.-J., Duan, S., Liu, H., McKee, B. A., Powell, R. T. & Stewart, C. M. 2005 Biogeochemical characteristics of the lower Mississippi River, USA, during June 2003. *Estuaries* **28**, 664–674. https://doi.org/10.1007/BF02732905.

Dean, W. E. & Gorham, E. 1998 Magnitude and significance of carbon burial in lakes, reservoirs, and peatlands. *Geology* **26**, 535–538. https://doi.org/10.1130/0091-7613(1998)026<0535:MASOCB > 2.3.CO;2.

de Montety, V., Martin, J. B., Cohen, M. J., Foster, C. & Kurz, M. J. 2011 Influence of diel biogeochemical cycles on carbonate equilibrium in a karst river. *Chemical Geology* **283**, 31–43. https://doi.org/10.1016/j.chemgeo.2010.12.025.

Ferris, F. G., Wiese, R. G. & Fyfe, W. S. 1994 Precipitation of carbonate minerals by microorganisms: implications for silicate weathering and the global carbon dioxide budget. *Geomicrobiology Journal* **12**, 1–13. https://doi.org/10.1080/01490459409377966.

Ford, D. & Williams, P. W. 1989 *Karst Geomorphology and Hydrology*. Chapman&Hall, London.

Friedlingstein, P., O'Sullivan, M., Jones, M. W., Andrew, R. M., Hauck, J., Olsen, A., Peters, G. P., Peters, W., Pongratz, J., Sitch, S., Le Quéré, C., Canadell, J. G., Ciais, P., Jackson, R. B., Alin, S., Aragão, L. E. O. C., Arneth, A., Arora, V., Bates, N. R., Becker, M., Benoit-Cattin, A., Bittig, H. C., Bopp, L., Bultan, S., Chandra, N., Chevallier, F., Chini, L. P., Evans, W., Florentie, L., Forster, P. M., Gasser, T., Gehlen, M., Gilfillan, D., Gkritzalis, T., Gregor, L., Gruber, N., Harris, I., Hartung, K., Haverd, V., Houghton, R. A., Ilyina, T., Jain, A. K., Joetzjer, E., Kadono, K., Kato, E., Kitidis, V., Korsbakken, J. I., Landschützer, P., Lefèvre, N., Lenton, A., Lienert, S., Liu, Z., Lombardozzi, D., Marland, G., Metzl, N., Munro, D. R., Nabel, J. E. M. S., Nakaoka, S.-I., Niwa, Y., O'Brien, K., Ono, T., Palmer, P. I., Pierrot, D., Poulter, B., Resplandy, L., Robertson, E., Rödenbeck, C., Schwinger, J., Séférian, R., Skjelvan, I., Smith, A. J. P., Sutton, A. J., Tanhua, T., Tans, P. P., Tian, H., Tilbrook, B., van der Werf, G., Vuichard, N., Walker, A. P., Wanninkhof, R., Watson, A. J., Willis, D., Wiltshire, A. J., Yuan, W., Yue, X. & Zaehle, S. 2020 Global Carbon Budget 2020. *Earth System Science Data* **12**, 3269–3340. https://doi.org/10.5194/essd-12-3269-2020.

Gaillardet, J., Dupré, B., Louvat, P. & Allègre, C. J. 1999 Global silicate weathering and CO_2 consumption rates deduced from the chemistry of large rivers. *Chemical Geology* **159**, 3–30. https://doi.org/10.1016/S0009-2541(99)00031-5.

Gombert, P. 2002 Role of karstic dissolution in global carbon cycle. *Global and Planetary Change* **33**, 177–184. https://doi.org/10.1016/S0921-8181(02)00069-3.

Gruber, N. & Galloway, J. N. 2008 An earth-system perspective of the global nitrogen cycle. *Nature* **451**, 293–296.

Gu, J., Yang, Q., Jiang, Z., Luo, W., Zeng, H., Qin, X. & Lan, F. 2018 Spatial variation analysis of soil carbon, nitrogen and phosphorus eco-stoichiometric ratios in karst and non-karst areas of Guangnan country, Yunnan, China. *Carsologica Sinica* **37**, 761–769.

Guo, F., Jiang, G. & Kang, Z. 2011 Study on carbon sink effect in typical sub-tropical karst water system. *Carsologica Sinica* **30**, 403–409.

Hartmann, A. 2015 Karst water resources in a changing world: review of hydrological modeling approaches. *Reviews of Geophysics* **52**, 218–242.

Holmes, R. M., McClelland, J. W., Peterson, B. J., Tank, S. E., Bulygina, E., Eglinton, T. I., Gordeev, V. V., Gurtovaya, T. Y., Raymond, P. A., Repeta, D. J., Staples, R., Striegl, R. G., Zhulidov, A. V. & Zimov, S. A. 2012 Seasonal and annual fluxes of nutrients and organic matter from large rivers to the Arctic ocean and surrounding seas. *Estuaries and Coasts* **35**, 369–382. https://doi.org/10.1007/s12237-011-9386-6.

Howarth, R. 2009 Nitrogen. In: *Encyclopedia of Inland Waters* (Likens, G. E., eds). Academic Press, Oxford, pp. 57–64. https://doi.org/10.1016/B978-012370626-3.00098-3.

Jiang, Z., Qin, X., Cao, J., Jiang, X., He, S. & Luo, W. 2011 Calulation of atmospheric CO_2 sink formed in karst progresses of the karst divided regions in China. *Carsologica Sinica* **30**, 363–367.

Jiang, Y. 2013 The contribution of human activities to dissolved inorganic carbon fluxes in a karst underground river system: evidence from major elements and δ13CDIC in Nandong, Southwest China. *Journal of Contaminant Hydrology* **152**, 1–11.

Jiang, Y., Hu, Y. & Schirmer, M. 2013 Biogeochemical controls on daily cycling of hydrochemistry and δ13C of dissolved inorganic carbon in a karst spring-fed pool. *Journal of Hydrology* **478**, 157–168. https://doi.org/10.1016/j.jhydrol.2012.12.001.

Jørgensen, N. O. G. 2009 Organic nitrogen. In: *Encyclopedia of Inland Waters* (Likens, G. E., eds). Academic Press, Oxford, pp. 832–851. https://doi.org/10.1016/B978-012370626-3.00119-8.

Kump, L. R., Brantley, S. L. & Arthur, M. A. 2000 Chemical weathering, atmospheric CO_2, and climate. *Annual Review of Earth and Planetary Sciences* **28**, 611–667. https://doi.org/10.1146/annurev.earth.28.1.611.

Lal, R. 2008 Carbon sequestration. *Philosophical Transactions of the Royal Society B: Biological Sciences* **363**, 815–830. https://doi.org/10.1098/rstb.2007.2185.

Li, J. & Zhang, J. 2003 Chemical weathering processes and atmospheric CO_2 consumption in the Yellow River drainage basin. *Marine Geology & Quaternary Geology* **02**, 43–49.

Li, Q., He, Y., Cao, J., Liang, J. & Zhu, M. 2011 The plant carbonic anhydrase at karst area and its ecological effects. *Ecology and Environmental Sciences* **20**, 1867–1871.

Li, C., Kang, S., Liu, Y., Hou, J., Guo, J., Liu, X., Cong, Z. & Zhang, Q. 2016 Distribution of major ions in waters and their response to regional climatic change in Tibetan lakes. *Journal of Lake Sciences* **28**, 743–754.

Li, H., Wang, S., Bai, X., Cao, Y. & Wu, L. 2019 Spatiotemporal evolution of carbon sequestration of limestone weathering in China. *Science China Earth Science* **62**, 974–991. https://doi.org/10.1007/s11430-018-9324-2.

Liu, Z. & Dreybrod, W. 1997 Dissolution kinetics of calcium carbonate minerals in H_2O-CO_2 solutions in turbulent flow: the role of the diffusion boundary layer and the slow reaction $H_2O + CO_2 \rightarrow H+ + HCO_3^-$. *Geochimica et Cosmochimica Acta* **61**, 2879–2889. https://doi.org/10.1016/S0016-7037(97)00143-9.

Liu, Z., Groves, C., Yuan, D., Meiman, J., Jiang, G., He, S. & Li, Q. 2004 Hydrochemical variations during flood pulses in the south-west China peak cluster karst: impacts of $CaCO_3$–H_2O–CO_2 interactions. *Hydrological Processes* **18**, 2423–2437. https://doi.org/10.1002/hyp.1472.

Liu, Z., Li, Q., Sun, H. & Wang, J. 2007 Seasonal, diurnal and storm-scale hydrochemical variations of typical epikarst springs in subtropical karst areas of SW China: soil CO_2 and dilution effects. *Journal of Hydrology* **337**, 207–223. https://doi.org/10.1016/j.jhydrol.2007.01.034.

Liu, Y., Zhang, J., He, Y., Sun, H. & Liu, Z. 2010a The utilization of dissolved inorganic carbon by Oocystic solitatia Wittr and its influence on the precipitation of calcium carbonate. *Geochimica* **39**, 191–196.

Liu, Z., Dreybrodt, W. & Wang, H. 2010b A new direction in effective accounting for the atmospheric CO_2 budget: considering the combined action of carbonate dissolution, the global water cycle and photosynthetic uptake of DIC by aquatic organisms. *Earth-Science Reviews* **99**, 162–172. https://doi.org/10.1016/j.earscirev.2010.03.001.

Liu, Z., Dreybrodt, W. & Liu, H. 2011 Atmospheric CO_2 sink: Silicate weathering or carbonate weathering? In: *Applied Geochemistry, Ninth International Symposium on the Geochemistry of the Earth's Surface (GES-9) 26*. pp. S292–S294. https://doi.org/10.1016/j.apgeochem.2011.03.085.

Liu, S. M., Li, L. W., Zhang, G. L., Liu, Z., Yu, Z. & Ren, J. L. 2012 Impacts of human activities on nutrient transports in the Huanghe (Yellow River) estuary. *Journal of Hydrology* **430–431**, 103–110. https://doi.org/10.1016/j.jhydrol.2012.02.005.

Liu, Z., Guan, D., Wei, W., Davis, S. J., Ciais, P., Bai, J., Peng, S., Zhang, Q., Hubacek, K., Marland, G., Andres, R. J., Crawford-Brown, D., Lin, J., Zhao, H., Hong, C., Boden, T. A., Feng, K., Peters, G. P., Xi, F., Liu, J., Li, Y., Zhao, Y., Zeng, N. & He, K.

2015 Reduced carbon emission estimates from fossil fuel combustion and cement production in China. *Nature* **524**, 335–338. https://doi.org/10.1038/nature14677.
Liu, Z., Macpherson, G., Groves, C., Martin, J. B., Yuan, D. & Zeng, S. 2018 Large and active CO2 uptake by coupled carbonate weathering. *Earth-Science Reviews* **182**, 42–49.
Liu, Q., Liang, Y., Cai, W.-J., Wang, K., Wang, J. & Yin, K. 2020 Changing riverine organic C:N ratios along the Pearl River: implications for estuarine and coastal carbon cycles. *Science of the Total Environment* **709**, 136052. https://doi.org/10.1016/j.scitotenv.2019.136052.
Liu, X., Zhou, Z., Zhang, H., Dan, Y. & Jiang, Y. 2021 Changes of hydrochemistry and dissolved inorganic carbon during thermal stratification in Pingzhai Reservoir. *Resources and Environment in the Yangtze Basin* **30**, 936–945.
Ma, S., Wei, Y., Han, C., Yan, H., Liu, Z., Sun, H. & Bao, Q. 2021 Hydrochemical characteristics in karst reservoir and its' implication for inorganic carbon deposition fluxes. *Journal of Lake Sciences* **33** (6), 1–14.
Martin, J. B. 2017 Carbonate minerals in the global carbon cycle. *Chemical Geology* **449**, 58–72. https://doi.org/10.1016/j.chemgeo.2016.11.029.
McLauchlan, K. K., Williams, J. J., Craine, J. M. & Jeffers, E. S. 2013 Changes in global nitrogen cycling during the Holocene epoch. *Nature* **495**, 352–355. https://doi.org/10.1038/nature11916.
Medinets, S., Skiba, U., Rennenberg, H. & Butterbach-Bahl, K. 2015 A review of soil NO transformation: associated processes and possible physiological significance on organisms. *Soil Biology and Biochemistry* **80**, 92–117.
Melnikov, N. B. & O'Neill, B. C. 2006 Learning about the carbon cycle from global budget data. *Geophysical Research Letters* **33**, L02705. https://doi.org/10.1029/2005GL023935.
Meybeck, M. 1982 Carbon, nitrogen, and phosphorus transport by world rivers. *American Journal of Science* **282**, 401–450.
Nie, S., Zhao, L., Lei, X., Sarfraz, R. & Xing, S. 2018 Dissolved organic nitrogen distribution in differently fertilized paddy soil profiles: implications for its potential loss. *Agriculture, Ecosystems & Environment* **262**, 58–64.
Nõges, P., Cremona, F., Laas, A., Martma, T., Rõõm, E.-I., Toming, K., Viik, M., Vilbaste, S. & Nõges, T. 2016 Role of a productive lake in carbon sequestration within a calcareous catchment. *Science of the Total Environment* **550**, 225–230.
Pedersen, O., Colmer, T. D. & Sand-Jensen, K. 2013 Underwater photosynthesis of submerged plants–recent advances and methods. *Frontiers in Plant Science* **4**, 140.
Pu, J., Li, J., Khadka, M. B., Martin, J. B., Zhang, T., Yu, S. & Yuan, D. 2017 In-stream metabolism and atmospheric carbon sequestration in a groundwater-fed karst stream. *Science of the Total Environment* **579**, 1343–1355. https://doi.org/10.1016/j.scitotenv.2016.11.132.
Qin, X., Jiang, Z., Zhang, L., Huang, Q. & Liu, P. 2015 The difference of the weathering rate between carbonate rocks and silicate rocks and its effects on the atmospheric CO_2 consumption in the Pearl River Basin. *Geological Bulletin of China* **34**, 1749–1757.
Rasilo, T., Hutchins, R. H. S., Ruiz-González, C. & del Giorgio, P. A. 2017 Transport and transformation of soil-derived CO_2, CH_4 and DOC sustain CO_2 supersaturation in small boreal streams. *Science of the Total Environment* **579**, 902–912. https://doi.org/10.1016/j.scitotenv.2016.10.187.
Raymond, P. A., Oh, N.-H., Turner, R. E. & Broussard, W. 2008 Anthropogenically enhanced fluxes of water and carbon from the Mississippi River. *Nature* **451**, 449–452. https://doi.org/10.1038/nature06505.
Sabine, C. L., Feely, R. A., Gruber, N., Key, R. M., Lee, K., Bullister, J. L., Wanninkhof, R., Wong, C. S., Wallace, D. W. R., Tilbrook, B., Millero, F. J., Peng, T.-H., Kozyr, A., Ono, T. & Rios, A. F. 2004 The oceanic sink for anthropogenic CO_2. *Science* **305**, 367–371. https://doi.org/10.1126/science.1097403.
Song, A., Peng, W., He, R., Jin, Z., Lu, X., Fang, J., Huang, B. & Li, Q. 2017 Hydrochemistry characteristics in front of the Wulixia Reservoir Dam associated with feedback from aerobic anoxygenic phototrophic bacteria. *Rock and Mineral Analysis* **36**, 171–179.
Song, X., Gao, Y., Green, S. M., Wen, X., Dungait, J. A. J., Xiong, B., Quine, T. A. & He, N. 2019 Rainfall driven transport of carbon and nitrogen along karst slopes and associative interaction characteristic. *Journal of Hydrology* **573**, 246–254. https://doi.org/10.1016/j.jhydrol.2019.03.083.
Sun, P., He, S., Yuan, Y., Yu, S. & Zhang, C. 2019 Effects of aquatic phototrophs on seasonal hydrochemical, inorganic, and organic carbon variations in a typical karst basin, Southwest China. *Environmental Science and Pollution Research* **26**, 32836–32851. https://doi.org/10.1007/s11356-019-06374-6.
Sun, P., He, S., Yu, S., Pu, J., Yuan, Y. & Zhang, C. 2021 Dynamics in riverine inorganic and organic carbon based on carbonate weathering coupled with aquatic photosynthesis in a karst catchment, Southwest China. *Water Research* **189**, 116658. https://doi.org/10.1016/j.watres.2020.116658.
Tortell, P. D., Payne, C., Gueguen, C., Strzepek, R. F., Boyd, P. W. & Rost, B. 2008 Inorganic carbon uptake by Southern Ocean phytoplankton. *Limnology and Oceanography* **53**, 1266–1278. https://doi.org/10.4319/lo.2008.53.4.1266.
Van Cappellen, P. & Qiu, L. 1997 Biogenic silica dissolution in sediments of the Southern Ocean. II. Kinetics. *Deep Sea Research Part II: Topical Studies in Oceanography* **44**, 1129–1149. https://doi.org/10.1016/S0967-0645(96)00112-9.
Wakida, F. T. & Lerner, D. N. 2005 Non-agricultural sources of groundwater nitrate: a review and case study. *Water Research* **39**, 3–16.
Wang, F., Wang, Y., Zhang, J., Xu, H. & Wei, X. 2007 Human impact on the historical change of CO_2 degassing flux in River Changjiang. *Geochemical Transactions* **8**, 7. https://doi.org/10.1186/1467-4866-8-7.

Wang, F., Wang, B., Liu, C.-Q., Wang, Y., Guan, J., Liu, X. & Yu, Y. 2011 Carbon dioxide emission from surface water in cascade reservoirs–river system on the Maotiao River, southwest of China. *Atmospheric Environment* **45**, 3827–3834. https://doi.org/10.1016/j.atmosenv.2011.04.014.

Wang, Q., Ma, M., Jiang, X., Guan, D., Wei, D., Zhao, B., Chen, S., Cao, F., Li, L. & Yang, X. 2019a Impact of 36 years of nitrogen fertilization on microbial community composition and soil carbon cycling-related enzyme activities in rhizospheres and bulk soils in northeast China. *Applied Soil Ecology* **136**, 148–157.

Wang, Y., Ying, H., Yin, Y., Zheng, H. & Cui, Z. 2019b Estimating soil nitrate leaching of nitrogen fertilizer from global meta-analysis. *Science of the Total Environment* **657**, 96–102.

Wei, X. 2003 *The Fluxes of Carbon and Erosion in Pearl River Delta*. PhD, Graduate School of Chinese Academy of Sciences.

Wu, Y., Zhang, J., Liu, S. M., Zhang, Z. F., Yao, Q. Z., Hong, G. H. & Cooper, L. 2007 Sources and distribution of carbon within the Yangtze River system. *Estuarine, Coastal and Shelf Science* **71**, 13–25. https://doi.org/10.1016/j.ecss.2006.08.016.

Wu, X., Song, Y., Wang, J., Gao, H., Liu, C. & Li, B. 2021 Groundwater hydrogeochemical characteristics in the up reaches of Chaiwen River, Shandong Province. *Environmental Chemistry* **40** (7), 1–10.

Xin, J., Liu, Y., Chen, F., Duan, Y., Wei, G., Zheng, X. & Li, M. 2019 The missing nitrogen pieces: a critical review on the distribution, transformation, and budget of nitrogen in the vadose zone-groundwater system. *Water Research* **165**, 114977. https://doi.org/10.1016/j.watres.2019.114977.

Yang, R., Sun, H., Chen, B., Yang, M., Zeng, Q., Zeng, C., Huang, J., Luo, H. & Lin, D. 2020 Temporal variations in riverine hydrochemistry and estimation of the carbon sink produced by coupled carbonate weathering with aquatic photosynthesis on land: an example from the Xijiang River, a large subtropical karst-dominated river in China. *Environmental Science and Pollution Research* **27**, 13142–13154. https://doi.org/10.1007/s11356-020-07872-8.

Yuan, D. 1997 Modern karstology and global change study. *Earth Science Frontiers* **4**, 21–29.

Yuan, D. & Liu, Z. 2003 *Carbon Cycle and Karst Geological Environment*. Sciences Press, Beijing.

Zeebe, R. E. & Caldeira, K. 2008 Close mass balance of long-term carbon fluxes from ice-core CO_2 and ocean chemistry records. *Nature Geoscience* **1**, 312–315. https://doi.org/10.1038/ngeo185.

Zeng, S., Liu, H., Liu, Z., Kaufmann, G., Zeng, Q. & Chen, B. 2019 Seasonal and diurnal variations in DIC, NO_3^- and TOC concentrations in spring-pond ecosystems under different land-uses at the Shawan Karst Test Site, SW China: carbon limitation of aquatic photosynthesis. *Journal of Hydrology* **574**, 811–821. https://doi.org/10.1016/j.jhydrol.2019.04.090.

Zhang, J., Huang, W. W., Létolle, R. & Jusserand, C. 1995 Major element chemistry of the Huanghe (Yellow River), China – weathering processes and chemical fluxes. *Journal of Hydrology* **168**, 173–203. https://doi.org/10.1016/0022-1694(94)02635-O.

Zhang, E., Wang, Y., Qian, Y., Ma, T., Zhang, D., Zhan, H., Zhang, Z., Fei, Y. & Wang, S. 2013a Iodine in groundwater of the North China Plain: spatial patterns and hydrogeochemical processes of enrichment. *Journal of Geochemical Exploration* **135**, 40–53. https://doi.org/10.1016/j.gexplo.2012.11.016.

Zhang, L. J., Wang, L., Cai, W.-J., Liu, D. M. & Yu, Z. G. 2013b Impact of human activities on organic carbon transport in the Yellow River. *Biogeosciences* **10**, 2513–2524. https://doi.org/10.5194/bg-10-2513-2013.

Zhang, L., Qin, X., Liu, P. & Huang, Q. 2016 Chemical denudation rate and atmospheric CO_2 consumption by H_2CO3 and H_2SO4 in the Yangtze River Catchment. *Acta Geologica Sinica* **90**, 1933–1944.

Zhang, Z., Chen, X., Cheng, Q., Li, S., Yue, F., Peng, T., Waldron, S., Oliver, D. M. & Soulsby, C. 2020 Coupled hydrological and biogeochemical modelling of nitrogen transport in the karst critical zone. *Science of The Total Environment* **732**, 138902. https://doi.org/10.1016/j.scitotenv.2020.138902.

Zhang, S., Bai, X., Zhao, C., Tan, Q., Luo, G., Wang, J., Li, Q., Wu, L., Chen, F., Li, C., Deng, Y., Yang, Y. & Xi, H. 2021 Global CO_2 consumption by silicate rock chemical weathering: its past and future. *Earth's Future* **9**. https://doi.org/10.1029/2020EF001938.

Zhao, H., Xiao, Q., Miao, Y., Wang, Z. & Wang, Q. 2020 Sources and transformations of nitrate constrained by nitrate isotopes and Bayesian model in karst surface water, Guilin, Southwest China. *Environmental Science and Pollution Research* **27**, 21299–21310.

Zhao, H., Jiang, Y., Xiao, Q., Zhang, C. & Behzad, H. M. 2021 Coupled carbon-nitrogen cycling controls the transformation of dissolved inorganic carbon into dissolved organic carbon in karst aquatic systems. *Journal of Hydrology* **592**, 125764. https://doi.org/10.1016/j.jhydrol.2020.125764.

Zhou, Y., Wang, Y., Li, Y., Zwahlen, F. & Boillat, J. 2013 Hydrogeochemical characteristics of central Jianghan Plain, China. *Environmental Earth Sciences* **68**, 765–778. https://doi.org/10.1007/s12665-012-1778-9.

Zigah, P. K., Minor, E. C. & Werne, J. P. 2012 Radiocarbon and stable-isotope geochemistry of organic and inorganic carbon in Lake Superior. *Global Biogeochemical Cycles* **26**. https://doi.org/10.1029/2011GB004132.

First received 5 November 2021; accepted in revised form 21 November 2021. Available online 3 December 2021